VISUALIZATION AND HEAT TRANSFER STUDY OF A SYNTHETIC JET IMPINGING ON A CIRCULAR CYLINDER

Broučková Z.* and Trávníček Z.
*Author for correspondence
Institute of Thermomechanics, the Czech Academy of Sciences,
Dolejškova 5, 182 00 Prague, Czech Republic,
E-mail: brouckova@it.cas.cz

ABSTRACT

The present study deals with a slot fluid jet impinging onto an electrically heated circular cylinder in water. The continuous and synthetic jets were tested. The slot nozzle width was 0.36 mm, the cylinder diameter was 1.2 mm, and the cylinder-to-nozzle spacing, related to the slot width, was 5–21. The Reynolds numbers based on the nozzle width ranged 35–170. The Laser-Induced Fluorescence (LIF) visualization revealed a dominant flow separation occurring on the windward cylinder side for both continuous and synthetic jets. The flow around the leeward cylinder side is completely absent. It is attributed to the effects of the mini scale and low Reynolds numbers. An increase of the Reynolds numbers changes flow pattern from a steady jet-flow separation to a vortex shedding wake-flow regime. Heat transfer experiments were validated in a natural convection regime. An enhancement of average Nusselt numbers by 4.2–6.2 times by means of the synthetic jets was quantified by comparison with the natural convection regime. A correlation for the average Nusselt number was proposed for both continuous and synthetic jets.

INTRODUCTION

Submerged *impinging jets* (IJs) and impingement heat transfer on exposed walls have been widely studied in the past. The most important early results were collected by Dyban and Mazur [1] and Martin [2]. Since then, several comprehensive reviews have appeared, e.g. [3, 4].

A majority of the IJ studies focused on jets impinging onto flat surfaces. A markedly smaller amount of the studies deals with slot jets impinging onto a cylinder. If a small cylinder is submerged into the potential core of a jet, the task can resemble a circular cylinder in a uniform cross flow – e.g. [5, 6]. If the cylinder diameter (D) is comparable with the slot width (B), a complex task occurs. A majority of available experimental studies are focused on Reynolds numbers of $Re_D > 10^3$ (where Re_D is defined as $Re_D = UD/\nu$, where U is the nozzle-exit mean velocity, and ν is the kinematic viscosity of the working fluid).

Only very few studies investigated slot jets impinging on circular cylinders at low Reynolds numbers ($Re_D < 10^3$), [7–9]. McDaniel and Webb [7] measured an average heat transfer in air at following parameters: D = 12.7 mm, B/D = 0.5–1.52, H/B = 1–11 (where H is the cylinder-to-nozzle spacing), and Re_D = 600–8 000. Three cases were distinguished, depending on positions of cylinders in jets: (A) Cylinder fully submerged into the jet potential core with relatively low heat transfer. (B) Cylinder located near the tip of the potential core. Heat transfer is enhanced because the shear layers generate high turbulence. The maximum heat transfer was found at the optimum value of H/B = 2–4. The average heat transfer coefficient is higher when compared to an infinite uniform cross-flow. (C) Cylinder positioned downstream of the potential core. A decay of the streamwise velocity there causes a gradual decrease of the heat transfer coefficient.

Note that these three flow field types (A, B, C) with the optimum at H/B = 2–4 are linked with relatively large orifices at B/D = 0.5–1.52 [7]. If the orifices are relatively smaller, McDaniel and Webb [7] speculated about another scenario: the average heat transfer coefficient is likely to be reduced. Two reasons of that reduction were suggested: the side portions of the cylinder can be outside the turbulent jet shear layers and the jet flow cannot reach a leeward side of a large cylinder.

NOMENCLATURE

B	[m]	width of the SJ slot nozzle, B = 0.36 mm, see Fig. 1
D	[m]	diameter of the cylinder, see Fig. 1
Gr		Grashof number
h	[W/(m^{2}K)]	average heat transfer coefficient
H	[m]	nozzle-to-wall spacing, see Fig. 1
I	[A]	electrical current for cylinder heating
IJ		impinging jet
k	[W/(m K)]	thermal conductivity of the working fluid (water)
L	[m]	length of the nozzle exit channel, see Fig. 1
L_C	[m]	total length of the cylinder, see Fig. 1
L_H	[m]	length of the cylinder test section, see Fig. 1
L_S	[m]	slot nozzle length, see Fig. 1
Nu		average Nusselt number, $Nu = h\,D/k$
P	[W]	electrical power input for cylinder heating, $P = IV$
Re_{CJ}		Reynolds number of continuous jet, $Re_{CJ} = UB/\nu$
Re_D		Reynolds number, $Re_D = UB/\nu$ for CJ, $Re_D = U_0B/\nu$ for SJ
$Re_{D,c}$		Reynolds number corrected for centerplane conditions
Re_{SJ}		Reynolds number of synthetic jet, $Re_{SJ} = U_0B/\nu$
Ri		Richardson number, $Ri = Gr/Re_D^2$
SJ		synthetic jet
t	[s]	time
T	[s]	time period
T_f	[°C]	film temperature, $T_f = (T_w+T_\infty)/2$
T_w	[°C]	cylinder wall temperature
T_∞	[°C]	fluid bulk temperature, identical with the jet temperature
u	[m/s]	velocity
u_0	[m/s]	centerline exit velocity of SJ
U_0	[m/s]	time-mean exit velocity of SJ
V	[V]	voltage difference over the cylinder test section
x, y, z	[m]	Cartesian coordinates, see Fig. 1
ν	[m^2/s]	kinematic viscosity of the working fluid (water)

More recently, Jeng et al. [9] investigated heat transfer characteristics of stationary and rotating cylinders in a slot IJs in air at D = 40 mm, B/D = 0.0625–0.50, H/B = 1–16, and Re_D = 655–60 237. Under the stationary cylinders, the average Nusselt numbers are slightly higher than that for the cylinders in an infinite uniform cross flow – in agreement with [7].

All the above described IJ studies used continuous, steady-flow fluid jets (CJs). Another alternative is a utilization of pulsating jets. The *synthetic jet* (SJ) is one of the pulsating jets, namely a fluid flow motion that is created during an oscillatory process of a fluid exchange between a cavity and its surroundings – Smith and Glezer [10]. The first SJ actuator, as we think of it today, was most likely a laboratory air-jet generator designed and used by Dauphinee in 1957 [11]. Since the end of the last century, this phenomenon has been the subject of intensive investigations, usually under the name of the SJ [10, 12, 13] or zero-net-mass-flux jet [14, 15] or the oscillatory vorticity generator [15]. Note that SJ can exist only if fluid oscillations overcome formation criteria [16–20].

SJs are promising alternatives for various applications of active flow control – see the recent extensive review edited by Mohseni and Mittal [13]. Another potential is a convective heat transfer. One of earlier studies was presented by Yassour et al. [21]. Since that time, SJs for cooling have been investigated by many authors [22–33]. Particularly up-and-coming SJ applications are in a micro scale, such as the cooling of highly loaded electronic components in microchannels – see [31, 32]. Very small (mini/micro) scales imply very low Reynolds numbers with prevailing laminar character of flow. However, SJs can introduce fluctuations (called "quasi-turbulent" flow, [31] or "pseudo-turbulence", [32]) in laminar flows inducing a desirable enhancement of heat transfer and flow mixing.

It is worthy of notice here that the microjet flows can exhibit a specific and unexpected behavior. Chang et. al [34] investigated air IJs from slots of the widths of 50, 100 and 200 μm. They concluded a "peculiar phenomenon" which is unknown in macro-scale jets, because the coherent structures, vortex formation and merging processes are completely absent in the microjets. A penetration of the microjets into surroundings is relatively deeper and the breakdown process occurred at higher $Re_{CJ} = UB/\nu$. An optimal nozzle-to-wall spacing H/B for the maximum heat transfer was found inversely proportional to Re_{CJ}. For example, a decrease of the Re_{CJ} from 640 to 20 caused an increase of the optimal H/B from 25 to 800. The upper value is 80 times larger than the optimal value of the macro-scale (turbulent) slot IJs, cf. [2].

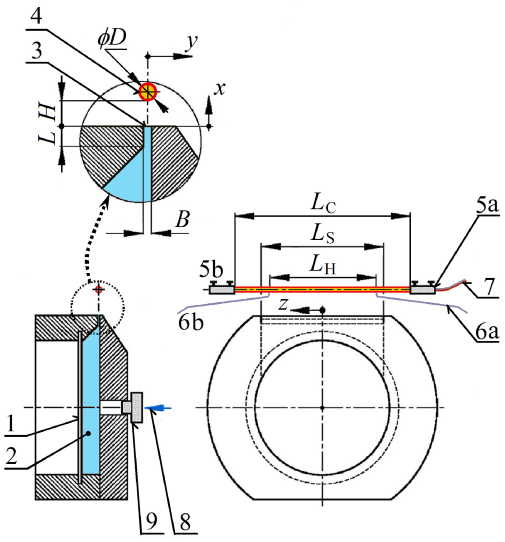

Figure 1 Experimental device

Slot jet impingement heat transfer from cylinders can be particularly promising in mini/micro scale applications. Utilizing of SJs for this purpose can be a very suitable alternative. To the best authors' knowledge a SJ impinging on a circular cylinder was not discussed in available literature until now. Therefore, a motivation of this study is to investigate an impingement heat transfer from a circular cylinder due to a slot SJ. The task is investigated at the mini scale in water.

EXPERIMENTAL INVESTIGATION

As written above, two Reynolds numbers play an important role in the task of a continuous jet impinging on a circular cylinder: $Re_D = UD/\nu$ and $Re_{CJ} = UB/\nu$. For SJs, the Reynolds numbers are defined consistently as $Re_D = U_0D/\nu$ and $Re_{SJ} = U_0B/\nu$, where U_0 is the time-mean exit velocity $U_0 = f\int_0^{T/2} u_0(t)\mathrm{d}t$ – see [10], where f is the frequency, $T = 1/f$ is the time period, and $u_0(t)$ is the centerline exit velocity.

The average Nusselt number is defined as $Nu = hD/k$, where h is the average heat transfer coefficient over the cylinder surface and k is the thermal conductivity of the fluid (water in this study). The k is evaluated at the film temperature $T_f = (T_w+T_\infty)/2$, where T_w is the cylinder wall temperature and T_∞ is the bulk temperature of the surrounding quiescent fluid which is coincident with the jet temperature at the slot exit.

Validation experiments were made by means of the natural convection. For this reason the Grashof number is defined as $Gr = g\beta(T_w-T_\infty)D^3/\nu^2$, where g is the acceleration of gravity, and β is the volumetric thermal expansion coefficient.

An influence of the mixed convection can be assumed as negligible. The forced convection criterion by Morgan [6] is used in the form of $Ri < 0.5$, where Ri is the Richardson number, $Ri = Gr/Re_D^2$. All experiments were performed at $Ri < 0.004$, thus the criterion was satisfied with great assurance.

Figure 1 shows a schematic view of the experimental device. The actuator body is made out of PMMA (polymethyl methacrylate). It is equipped with a piezoelectric diaphragm (position 1 in Fig. 1), which is the piezoceramic transducer KPS-l00 with the diaphragm diameter of D_D = 39.5 mm. The cavity (2) diameter and depth are 44 mm and 6 mm, respectively. The jet issues from a slot (3) on the top of the actuator. The slot width and length are B = 0.36 mm and L_s = 40 mm, respectively, i.e. the aspect ratio of the slot is L_s/B = 111. The length of the nozzle exit channel is L = 1.0 mm. The actuator coordinate system x, y, z is also shown in Fig. 1.

The described actuator can operate in two regimes to produce either CJ or SJ. In the CJ regime, a water inflow is fed into the actuator inlet (pos. 8) using a centrifugal pump. In the

SJ regime, the inlet is closed by a plug (9) and the diaphragm is driven by a sinusoidal current from a sweep/function generator (Agilent 33210A), which is amplified by an amplifier (RH Sound ST2250BC). Following the previous study [35], a near-resonance frequency of f = 46.4 Hz is used with the RMS voltage of 18.0 V. The power input and power factor were 9.5–12.2 mW and 0.80–0.86, respectively.

The cylinder (pos. 4) is made from a smooth stainless steel tube, its outside and inside diameters are D = 1.21 mm and 0.91 mm, respectively. The cylinder is mounted horizontally by two metal brackets (5a, 5b). The total cylinder length between the brackets is L_C = 57.5 mm. The cylinder is heated by the Joule effect of direct current I from these brackets. The maximum current was 9.5 A. The middle part of the cylinder is the test section, which is defined by the contact points with the span of L_H = 35.3 mm. The voltage difference V between these points is measured via a stainless steel wires of diameter 0.20 mm (6a, 6b), welded onto the cylinder surface in these contact points. The cylinder end-parts out of the test section operate as the end-guard sections. This arrangement minimizes axial conduction heat losses from the test section.

The experiments were made in a glass water tank with the following dimensions: height × length × depth = 150 × 245 × 140 mm. The working fluid is purified, demineralized and degasified water, which was prepared in four-stage reverse osmosis water purification system.

The LIF technique is based on the fluorescence effect. A solution of Rhodamine B is inserted into the water. The dye-stained flow was lit by the laser sheet (Nd:Yag pulsed laser, Litron, NANO S 65-15, with a wavelength of 532 nm and 65 mJ output, with cylindrical optics). The flow field pictures were taken using digital camera (HiSense Neo, 2560 × 2160 pixels, 16 bit) equipped with the lens (Tokina 100 mm F2.8 Macro D) and the colour filter (cut-off wavelength 570 nm). The system was controlled by DynamicStudio v3.40 Software (Dantec Dynamics). More details were described previously [36].

The time-mean exit velocities U of CJs and relating values of Re_{CJ} were quantified from the time-mean volume flux, which was measured by means of precise scales (Mettler Toledo PR 8002 Delta Range), similarly as in the study [36].

The heat generation rate within the cylinder test section is given by the electrical power input $P = IV$. Assuming a stationary regime (experiments were always performed after stabilization of all measured parameters), the thermal equilibrium of the test section can be expresses as $P=P_{CONV}+P_{RAD}+P_{COND}$, where P_{CONV}, P_{RAD} and P_{COND} are the convective, conductive, and radiation heat-transfer rates, respectively. The convective heat-transfer rate can be expressed as $P_{CONV} = hA(T_w - T_\infty)$, where A is the surface of the cylinder test section, $A = \pi D L_H$. Because the P_{RAD} and P_{COND} are negligible, the thermal equilibrium yields $Nu_D = P/[\pi k L_H (T_w - T_\infty)]$.

The thermal boundary condition at the cylinder surface is approximately uniform heat flux. To specify it more precisely, the differences of T_w along the cylinder span have to be taken into account. Because of typical saddle-back velocity profiles of the jets, which were found previously (see Fig. 2, [36]), the cylinder temperature slightly varied along the span. The maximum difference 3°C was evaluated, which caused less than 0.3% difference in heat flux. It is considered as negligible.

The cylinder temperature T_w was measured by a J type thermocouple and thermometer Omega DP41-B. The thermocouple was plugged into the cylinder tube – see pos. 7 in Fig. 1. The T_∞ was measured by an NTC thermistor sensor (Ahlborn AMR, Therm 2280-3). The maximum uncertainty of the current and voltage measurement is less than ±0.3 %, and ±0.5 %, respectively. The thermometers with probes had been calibrated and the maximum uncertainties of the T_w and T_∞ are less than ±0.2°C and ±0.1°C, respectively. The uncertainty of the Nu was evaluated within 5% with 95% confidence level.

RESULTS AND DISCUSSION

The CJ experiments are made in the range of U = 0.10–0.41 m/s which corresponds to Re_{CJ} = 40–171 and Re_D = 136–574. Fig. 2 shows a typical saddle-back velocity profile of CJ, which was measured previously by PIV at U = 0.12 m/s and Re_{CJ} = 45, [36]. The SJ experiments are made for U_0 = 0.21 m/s and Re_{SJ} = 79, as was quantified by LDV in the previous study [35].

Figure 3 and 4 show results of the LIF visualization of CJs and SJs, respectively. Originally, the laser sheet was in x-y plane [35, 36]. The present visualization uses a declination about 15° of the laser sheet from the x-y plane. It allows an observation in axonometric views in Figs. 3 and 4. For the sake of readability, the cylinder axis is plotted by a dash-and-dot line and the cylinder cross section is plotted too. The coordinates x, y, z are also shown. The spacing was adjusted as H = 20.8 B.

Figure 3(a) and 3(b) demonstrates the Reynolds number effect for an increase from the Re_D = 161 (i.e. Re_{CJ} = 48) in Fig. 3(a) to Re_D = 483 (i.e. Re_{CJ} = 144) in Fig. 3(b). The cylinder is unheated, $T_w = T_\infty$. For lower Re_D in Fig. 3(a), the CJ impinges on the cylinder. Then the jet is divided into two halves. A flow separation occurs very soon on the windward cylinder side. Finally, the flow leaves the cylinder in two halves forming a Y-shaped pattern. The flow around the leeward cylinder side is completely absent – this fact indicates a highly probable decrease in overall heat transfer rate. On the other hand, the flow pattern is basically different for higher Re_D as is shown in Fig. 3(b). Unlike Fig. 3(a), the flow around the leeward cylinder side exists in Fig. 3(b). The flow pattern resembles a vortex shedding wake known for cylinders in crossflow.

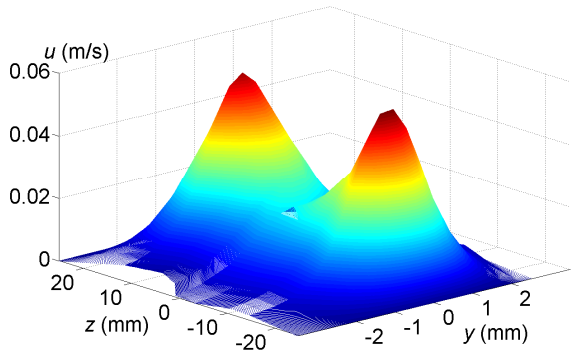

Figure 2 Streamwise velocity map of CJ at x/B = 30, [36]

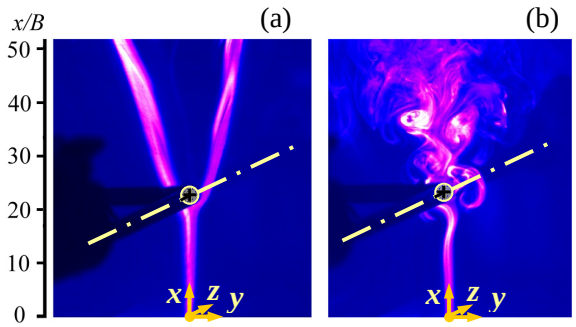

Figure 3 LIF visualization of CJs, unheated cases at $T_w = T_\infty$ and $H/B = 20.8$ for (a) $Re_D = 161$, (b) $Re_D = 483$

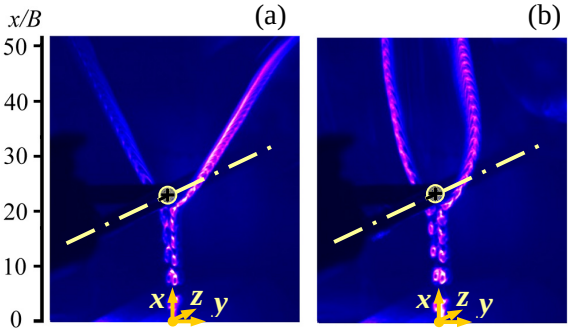

Figure 4 LIF visualization of SJs, $Re_{SJ} = 63$, $H/B = 20.8$, (a) unheated case, (b) heated case at T_w=28.4°C, T_∞=22.8°C

It is worth mentioning here another effect which is clearly manifested in Fig. 3(b), namely a low-frequency side-to-side motion of CJ before the front stagnation line. A frequency of these self-sustained oscillations was estimated approximately 1–2 Hz. Obviously, a deeper discussion of this sweeping-jet effect is beyond the scope of this study.

Figures 4(a) and 4(b) show a SJ impinging on a circular cylinder for unheated and heated cylinder cases, respectively. For the unheated case in Fig. 4(a), the Reynolds numbers are $Re_{SJ} = 63$ and $Re_D = 210$. For the heated case in Fig. 4(b), the Re_{SJ} is the same and for Fig. 4(a) and the temperatures are $T_w = 28.4$°C and $T_\infty = 22.8$°C. For both cases, the SJ impinges on the cylinder surface and it is divided into two halves. A flow separation occurs very soon on the windward cylinder side. Finally, the flow leaves the cylinder in two halves forming a Y-shaped pattern. The flow around the leeward cylinder side is completely absent. All this behavior is similar with that of CJ at lower Re_D, cf. Fig. 3(a).

Note some specific feature of the heated cylinder case in Fig. 4(b). While the both branches of the Y- shaped flow leaving the cylinder for unheated cases of Figs. 3(a), 4(a) are straight and directed nearly tangentially from the cylinder surface, these flow branches from heated cylinder in Fig. 4(b) are curved towards each other. This thermal effect in the far field indicates a thermal plume which is released from the leeward cylinder side, where the forced jet flow does not reach.

For validation purposes, an experiment under a natural convection regime was performed. The result is plotted in Fig. 5. Experimental correlations according to three representative studies [5, 6, 37] are shown in Fig. 5 too. The present data correspond very well to these correlations. Moreover, the correlation [6] is plotted including its declared maximum uncertainty of ±5% and Fig. 5 demonstrates that all present data are within this ±5% uncertainty range.

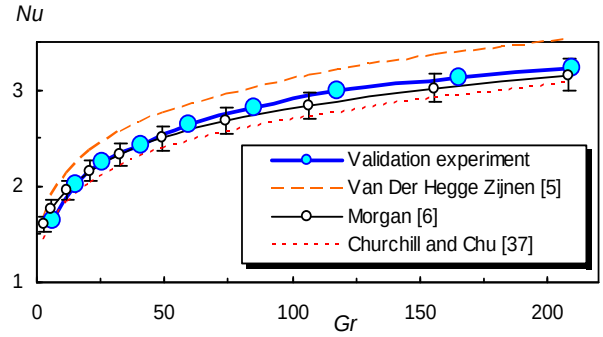

Figure 5 Natural convection - validation experiment

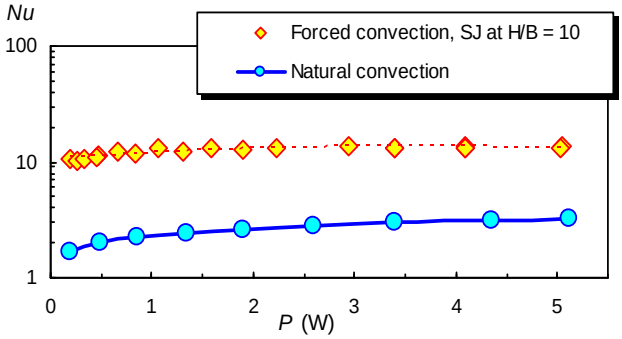

Figure 6 Comparison of natural and forced convection

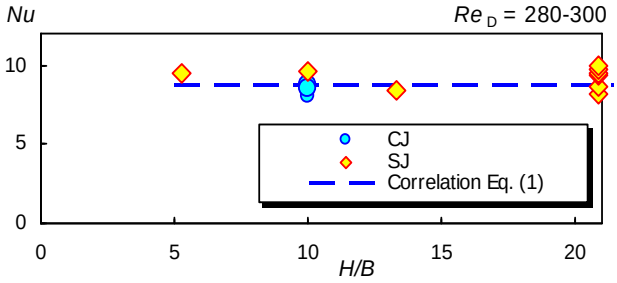

Figure 7 Effect of the nozzle-to-cylinder spacing on *Nu*

Figure 6 demonstrates heat transfer enhancement by mean of SJ at $H/B = 10$. A comparison of natural and forced convective heat transfer shows that the Nusselt numbers are 4.2–6.2 times higher for the forced convection with SJs.

Figure 7 shows the forced convection data for $Re_D = 280$–300. An effect of the nozzle-to-cylinder spacing H/B on *Nu* seems to be negligible, which agrees with literature for low Re_D – cf. Jeng et al. [9] for $Re_D < 1300$. To complete Fig. 7, the dashed line representing Eq. (1) is plotted too.

Figure 8(a) shows the present forced convection data in the

Nu-Re_D relationship. For comparison purposes, two references are used relating to the heat transfer from a circular cylinder to a uniform cross flow (Morgan [6]) and to an IJ (Amiri et al. [8]). The Nusselt numbers for CJ and SJ were evaluated from temperature T_w, which was measured at the center plane $z = 0$. Besides, the data series labeled as "CJ, near-end data" uses Nu evaluation from T_w, which was measured at the end of the cylinder test section where the local maximum of CJ velocity occurs, see Fig. 2 at $z = -15$ mm. Obviously, the near-end Nu values are higher than Nu values for center plane. The reason is the mentioned saddle-back velocity profile - in comparison with the mean exit velocity U, the mean centerplane exit velocity is smaller while the near-end exit velocity is higher. To quantify this effect, the $c(z)$ factor is defined as the ratio of the mean exit velocity in z location to the mean exit velocity U, i.e. $c(z) = L_S[\int u(y, z)dy]/U$. This factor was evaluated for velocities from Fig. 2 at $x/B = 10$–40 for z- locations at the centerplane $z = 0$ and the near-end plane $z = 15$ mm. The resulting values are $c(z=0) = 0.76 \pm 0.06$ and $c(z=15\text{mm}) = 1.55 \pm 0.06$. The c factor was used to make corrections of the Reynolds numbers for the centerplane conditions: $Re_{CJ,c} = c\ Re_{CJ}$ and $Re_{D,c} = c\ Re_D$.

Considering these described corrections, the results from Fig. 8(a) are replotted in Fig. 8(b) as the Nu-$Re_{D,c}$ relationships. By using the least-squares fitting, the results were correlated as

$$Nu = 0.63\ Re_{D,c}^{0.49} \qquad (1)$$

for $Re_{D,c}$ = 110–830. The maximum and standard deviation of experimental data from Eq. (1) are 13% and 7%, respectively.

Figure 8(b) demonstrates similar slopes of all correlation lines, i.e. a qualitative agreement of the present data with correlation by Morgan [6] (who proposed the exponent of 0.471). However, the present Nu values are much smaller than the results [6], namely 50.5% of [6]. The present smaller Nu values are a manifestation of the above discussed flow patterns when only a relatively small windward side the cylinder circumference is effectively cooled by the jet – see flow visualizations in Figs. 3 and 4. The reasons are a mini-scale effect of a narrow slot ($B = 0.36$ mm), relatively small ratio of B/D, and relatively low Re_D with prevailing laminar character of flow. However, the choice of small values of B, B/D and Re_D follows requirements of potential applications in mini/micro scales. Despite this choice reduces the Nusselt number in comparison with a cylinder in an infinite uniform cross-flow, it significantly saves the volume flux of the cooling fluid. A small volume flux is a principal capability of very compact, piezoelectric-driven actuators. A scaling down of this alternative seems to be possible more easily that of classical, compressor-driven macro scale devices [6, 8].

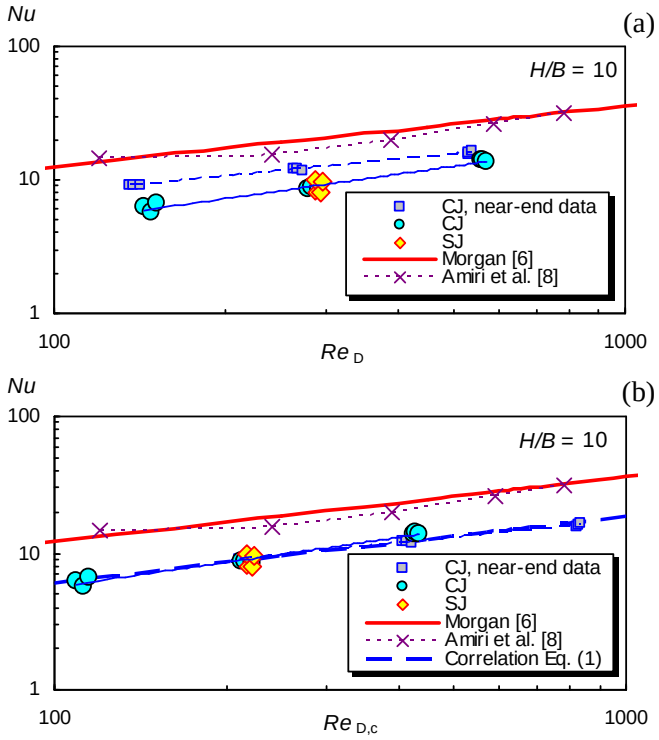

Figure 8 Overall heat transfer (a) Nu-Re_D, (b) Nu-$Re_{D,c}$

CONCLUSION

Slot fluid jets (namely continuous and synthetic jets) impinging onto an electrically heated circular cylinder were investigated in water. The LIF visualization revealed a steady flow separation on the windward cylinder side. For both continuous and synthetic jets, only a small front cylinder portion is effectively cooled by the jet while the flow around its leeward side is completely absent. An increase of the Reynolds numbers causes a qualitative change: a steady flow separation is replaced by a pattern resembling a vortex shedding wake.

Heat transfer experiments were validated by means of a natural convection regime and a very good agreement of the present results with representative literature was concluded. A meaningful augmentation by means of the synthetic jets was demonstrated: the Nu was enhanced 4.2–6.2 times in comparison with the natural convection regime. An effect of the nozzle-to-cylinder spacing on the Nu is negligible, which agrees with literature for lower Reynolds numbers.

Finally, the average Nusselt number was correlated by the relationship of $Nu = 0.63\ Re_{D,c}^{0.49}$, where $Re_{D,c}$ is the Reynolds number corrected for the centerplane flow conditions. The proposed exponent 0.49 well agrees with literature. On the other hand, the present Nu values are much smaller than the results known from macro scales (about 50%). The reasons are a mini-scale effect and low Reynolds numbers. However, the present choice of a narrow slot nozzle follows requirements of potential applications in mini/micro scales. It significantly saves the volume flux of the cooling fluid, therefore the actuator can be a very compact piezoelectric-driven device, with a promising possibility for a scale-down process.

Acknowledgments

We gratefully acknowledge the support of the GACR – Czech Science Foundation (projects no. 14-08888S and 16-16596S) and the institutional support RVO: 61388998.

REFERENCES

[1] Dyban E.P., and Mazur A.I., Convection Heat Transfer in Impinging Jets (Konvektivnyj teploobmen pri strujnom obtekanii tel), 1st ed., Naukova dumka, Kiev, 1982 (in Russian).

[2] Martin H., Heat and mass transfer between impinging gas jets and solid surfaces, *Advances in Heat Transfer*, Vol. 13, 1977, pp. 1–60.

[3] Webb B.W., and Ma C-F., Single-phase liquid jet impingement heat transfer, *Advances in Heat Transfer*, Vol. 26, 1995, pp. 105-107

[4] Garimella S.V., Heat transfer and flow fields in confined jet impingement, *Annual Review of Heat Transfer*, Vol. XI, 2000, pp. 413–494.

[5] Van Der Hegge Zijnen B. G, Modified correlation formulae for the heat transfers by natural and by forced convection from horizontal cylinders. *Applied Scientific Research*, Section A, Vol. 6, Issue 2, 1956, pp. 129–140.

[6] Morgan V. T., The overall convective heat transfer from smooth circular cylinders, *Advances in Heat Transfer*, Vol, 11, 1975, pp. 199–264.

[7] McDaniel C.S., and Webb B.W., Slot jet impingement heat transfer from circular cylinder. *International Journal of Heat and Mass Transfer*, Vol. 43, 2000, pp. 1975–1985.

[8] Amiri S., Habibi K., Faghani E., and Ashjaee M., Mixed convection cooling of a heated circular cylinder by laminar upward-directed slot jet impingement. *Heat Mass Transfer*, Vol. 46, 2009, pp. 225–236.

[9] Jeng T.-M., Tzeng S.-C., and Xu R., Heat transfer characteristics of a rotating cylinder with a lateral air impinging jet. *International Journal of Heat and Mass Transfer*, Vol. 70, 2014, pp. 235–249.

[10] Smith B.L., and Glezer A., The formation and evolution of synthetic jets, *Physics of Fluids*, Vol. 10, 1998, pp. 2281– 2297.

[11] Dauphinee, T.M., Acoustic air pump, *Review of Scientific Instruments*, Vol. 28, No. 6, 1957, p. 456.

[12] Mallinson S.G., Reizes J.A., and Hong G., An experimental and numerical study of synthetic jet flow, *The Aeronautical Journal*, Vol. 105, No. 1043, 2001, pp. 41–49.

[13] Mohseni K., and Mittal R., Synthetic Jets, Fundamentals and Applications. CRC Press, Taylor & Francis, Boca Raton, 2015.

[14] Cater J.E., and Soria J., The evolution of round zero-net-mass-flux jets, *Journal of Fluid Mechanics*, Vol. 472, 2002, pp. 167–200.

[15] Yehoshua T., and Seifert A., Boundary condition effects on the evolution of a train of vortex pairs in still air, *The Aeronautical Journal*, Vol. 110, 2006, pp. 397–417.

[16] Holman R., Utturkar Y., Mittal R., Smith B.L., and Cattafesta L., Formation criterion for synthetic jets, *AIAA Journal*, Vol. 43, No. 10, 2005, pp. 2110–2116.

[17] Zhou J., Tang H., and Zhong S., Vortex roll-up criterion for synthetic jets, *AIAA Journal*, Vol. 47, 2009, pp. 1252–1262.

[18] Trávníček Z., Broučková Z., and Kordík J., Formation criterion for axisymmetric synthetic jets at high Stokes numbers, *AIAA Journal*, Vol. 50, 2012, pp. 2012–2017.

[19] Xia Q., Zhong S., An experimental study on the behaviours of circular synthetic jets at low Reynolds numbers, *Proceedings of the Institution of Mechanical Engineers, Part C: Journal of Mechanical Engineering Science*, Vol. 226, 2012, pp. 2686–2700.

[20] Trávníček Z., Broučková Z., Kordík J., and Vít T., Visualization of synthetic jet formation in air, *Journal of Visualization*, Vol. 18, 2015, pp. 595–609.

[21] Yassour Y., Stricker J., and Wolfshtein M., Heat transfer from a small pulsating jet, *Proceedings of the 8th International Heat Transfer Conference*, Vol. 3, Hemisphere Publ., San Francisco, USA, 1986, pp. 1183–1186.

[22] Trávníček Z., and Tesař V., Annular synthetic jet used for impinging flow mass–transfer, *International Journal of Heat and Mass Transfer*, Vol. 46, No. 17, 2003, pp. 3291–3297.

[23] Kercher D.S., Lee J-B., Brand O., Allen M.G., and Glezer A., Microjet cooling devices for thermal management of electronics, *IEEE Tranaction on Components and Packaging Technologies*, Vol. 26, No. 2, 2003, pp. 359–366.

[24] Mahalingam R., Rumigny N., Glezer A., Thermal management using synthetic jet ejectors, *IEEE Transaction on Components and Packaging Technologies*, Vol. 27, No. 3, 2004, pp. 439–444.

[25] Gillespie, M.B., Black, W.Z., Rinehart, C., and Glezer, A., Local convective heat transfer from a constant heat flux flat plate cooled by synthetic air jets, *Journal of Heat Transfer-Transactions of the ASME*, Vol. 128, No. 10, 2006, pp. 990–1000.

[26] Arik M., An investigation into feasibility of impingement heat transfer and acoustic abatement of meso scale synthetic jets, *Applied Thermal Engineering*, Vol. 27, 2007, pp. 1483–1494.

[27] Chaudhari M., Puranik B., and Agrawal A., Heat transfer characteristics of synthetic jet impingement cooling, *International Journal of Heat and Mass Transfer*, Vol. 53, No. 5–6, 2010, pp. 1057–1069.

[28] Persoons T., McGuinn A., and Murray D.B., A general correlation for the stagnation point Nusselt number of an axisymmetric impinging synthetic jet, *International Journal of Heat and Mass Transfer*, Vol. 54, 2011, pp. 3900–3908.

[29] Trávníček Z., Tesař V., Broučková Z., and Peszyński K., Annular impinging jet controlled by radial synthetic jets, *Heat Transfer Engineering*, Vol. 35, No. 4, 2014, pp. 1450–1461.

[30] Trávníček Z., and Vít T., Impingement heat/mass transfer to hybrid synthetic jets and other reversible pulsating jets. *International Journal of Heat and Mass Transfer*, Vol. 85, 2015, pp. 473–487.

[31] Timchenko V., Reizes J.A., and Leonardi E., An evaluation of synthetic jets for heat transfer enhancement in air cooled micro-channels, *International Journal of Numerical Methods for Heat & Fluid Flow*, Vol. 17, No. 3, 2007, pp. 263–283.

[32] Lee A., Yeoh G.H., Timchenko V., and Reizes J.A., Flow structure generated by two synthetic jets in a channel: effect of phase and frequency, *Sensors and Actuators A: Physical*, Vol. 184, 2012, pp. 98–111.

[33] Trávníček Z., Dančová P., Kordík J., Vít T., and Pavelka M., Heat and mass transfer caused by a laminar channel flow equipped with a synthetic jet array, *Journal of Thermal Science and Engineering Applications-Transactions of the ASME*, Vol. 2, No. 4, 2010, pp. 041006-1–041006-8.

[34] Chang C.J., Chen H.T., and Gau C., Flow and heat transfer of a microjet impinging on a heated chip. Part II – heat transfer. *Nanoscale and Microscale Thermophysical Engineering*, Vol. 17, 2013, pp. 92–111.

[35] Broučková Z., Vít T., and Trávníček Z., Laser Doppler vibrometry experiment on a piezo-driven slot synthetic jet in water. The European Physical Journal, *EPJ Web of Conferences*, Vol. 92, 2015, Article No. 02007.

[36] Broučková Z., Hsu S.-S., Wang A.-B., and Trávníček Z., PIV and LIF study of slot continuous jet at low Reynolds number. *Proceedings of the International Conference Experimental Fluid Mechanics*, Prague, CR, Nov. 17–20, 2015, pp. 86–91.

[37] Churchill S.W., and Chu H.H.S, Correlating equations for laminar and turbulent free convection from a horizontal cylinder. *International Journal of Heat and Mass Transfer*, Vol. 18, 1975, pp. 1049–1053.